TATION PAGE

Form Approved
OMB No. 0704-0188

1. AGENCY USE ONLY (Leave blank)	2. REPORT DATE	3. REPORT TYPE AND DATES COVERED
	August 1991	Final - December 1990 to March 1991

4. TITLE AND SUBTITLE
Sixteen Lead Electrocardiographic Changes with Coronary Angioplasty - Location of STT Changes with Balloon Occlusion of Five Arterial Perfusion Beds

5. FUNDING NUMBERS
C - F33615-87-D-0609/0034
PE - 62202F
PR - 7755
TA - 27
WU - 21

6. AUTHOR(S)
Helge A. Saetre, Ronald H. Startt-Selvester, Joseph C. Solomon, Kesaag A. Baron, Javed Ahmed, and Myrvin E. Ellestad

7. PERFORMING ORGANIZATION NAME(S) AND ADDRESS(ES)
Southeastern Center for Electrical Engineering Education (SCEEE)
11th and Massachusetts Avenues
St Cloud, FL 34769

8. PERFORMING ORGANIZATION REPORT NUMBER

9. SPONSORING/MONITORING AGENCY NAME(S) AND ADDRESS(ES)
Clinical Sciences Division
Aerospace Medicine Directorate
USAF Armstrong Laboratory
Brooks Air Force Base

10. SPONSORING/MONITORING AGENCY REPORT NUMBER
AL-JA-1991-0052

11. SUPPLEMENTARY NOTES
USAF AL Technical Monitor: R. Brian Howe (512) 536-2285

12a. DISTRIBUTION/AVAILABILITY STATEMENT
Approved for public release; distribution is unlimited.

12b. DISTRIBUTION CODE

13. ABSTRACT (Maximum 200 words)
Percutaneous transluminal coronary angioplasty (PTCA) occlusion in 5 individual coronary artery distributions produced significant ST elevation ("current of injury") in 48/50 PTCAs in 46 patients. Four patients had PTCA of two separate coronary arteries. Two patients had no significant ischemic ST changes in the 16SL ECG and no chest pain with PTCA. The 6 limb leads were recorded from Mason-Likar locations modified by moving them centrally on the anterior torso; the V leads were recorded in standard locations, except VI was moved to V3R; 4 extra leads were placed as follows: 1) left axilla, 2) left subcostal margin, 3) V8, and 4) mild-back at the level of V4-V8. The left axillary and back leads discriminated diagonal and left circumflex (LCX) PTCAs from the others and from each other. V6 showed ST elevation in all LCX PTCAs and in only 10% of left anterior descending occlusions. V3R had ST elevation in 82% of right coronary PTCAs. In 48/50 (96%) of PTCA occlusions the ST elevation localized to the torso locations defined in Forward Model Simulations as specific for the arterial perfusion bed involved. These data strongly support the hypothesis that additional resolution and sensitivity to ischemic change is to be expected with a broader array of ECG leads.

14. SUBJECT TERMS
Electrocardiography, Coronary Artery Disease, Myocardial Ischemia, ST changes, ECG Forward Model

15. NUMBER OF PAGES

16. PRICE CODE

17. SECURITY CLASSIFICATION OF REPORT	18. SECURITY CLASSIFICATION OF THIS PAGE	19. SECURITY CLASSIFICATION OF ABSTRACT	20. LIMITATION OF ABSTRACT
Unclassified	Unclassified	Unclassified	UL

GENERAL INSTRUCTIONS FOR COMPLETING SF 298

The Report Documentation Page (RDP) is used in announcing and cataloging reports. It is important that this information be consistent with the rest of the report, particularly the cover and title page. Instructions for filling in each block of the form follow. It is important to **stay within the lines to meet optical scanning requirements.**

Block 1. Agency Use Only (Leave Blank)

Block 2. Report Date. Full publication date including day, month, and year, if available (e.g. 1 Jan 88). Must cite at least the year.

Block 3. Type of Report and Dates Covered. State whether report is interim, final, etc. If applicable, enter inclusive report dates (e.g. 10 Jun 87 - 30 Jun 88).

Block 4. Title and Subtitle. A title is taken from the part of the report that provides the most meaningful and complete information. When a report is prepared in more than one volume, repeat the primary title, add volume number, and include subtitle for the specific volume. On classified documents enter the title classification in parentheses.

Block 5. Funding Numbers. To include contract and grant numbers; may include program element number(s), project number(s), task number(s), and work unit number(s). Use the following labels:

C	- Contract	**PR**	- Project
G	- Grant	**TA**	- Task
PE	- Program Element	**WU**	- Work Unit Accession No.

Block 6. Author(s). Name(s) of person(s) responsible for writing the report, performing the research, or credited with the content of the report. If editor or compiler, this should follow the name(s).

Block 7. Performing Organization Name(s) and Address(es). Self-explanatory.

Block 8. Performing Organization Report Number. Enter the unique alphanumeric report number(s) assigned by the organization performing the report.

Block 9. Sponsoring/Monitoring Agency Names(s) and Address(es). Self-explanatory.

Block 10. Sponsoring/Monitoring Agency. Report Number. (If known)

Block 11. Supplementary Notes. Enter information not included elsewhere such as: Prepared in cooperation with...; Trans. of ..., To be published in .... When a report is revised, include a statement whether the new report supersedes or supplements the older report.

Block 12a. Distribution/Availablity Statement. Denote public availability or limitation. Cite any availability to the public. Enter additional limitations or special markings in all capitals (e.g. NOFORN, REL, ITAR)

DOD	- See DoDD 5230.24, "Distribution Statements on Technical Documents."
DOE	- See authorities
NASA	- See Handbook NHB 2200.2.
NTIS	- Leave blank.

Block 12b. Distribution Code.

DOD	- DOD - Leave blank
DOE	- DOE - Enter DOE distribution categories from the Standard Distribution for Unclassified Scientific and Technical Reports
NASA	- NASA - Leave blank
NTIS	- NTIS - Leave blank.

Block 13. Abstract. Include a brief (Maximum 200 words) factual summary of the most significant information contained in the report.

Block 14. Subject Terms. Keywords or phrases identifying major subjects in the report.

Block 15. Number of Pages. Enter the total number of pages.

Block 16. Price Code. Enter appropriate price code (NTIS only).

Blocks 17. - 19. Security Classifications. Self-explanatory. Enter U.S. Security Classification in accordance with U.S. Security Regulations (i.e., UNCLASSIFIED). If form contains classified information, stamp classification on the top and bottom of the page.

Block 20. Limitation of Abstract. This block must be completed to assign a limitation to the abstract. Enter either UL (unlimited) or SAR (same as report). An entry in this block is necessary if the abstract is to be limited. If blank, the abstract is assumed to be unlimited.

16-Lead ECG Changes With Coronary Angioplasty

Location of ST-T Changes With Balloon Occlusion of Five Arterial Perfusion Beds

Helge A. Saetre, MD, Ronald H. Startt/Selvester, MD, Joseph C. Solomon, MS, Keesag A. Baron, MD, Javed Ahmad, MD, and Myrvin E. Ellestad, MD

Abstract: Percutaneous transluminal coronary angioplasty (PTCA) occlusion in five individual coronary artery distributions produced significant ST elevation ("current of injury") in 48/50 PTCAs in 46 patients. Four patients had PTCA of two separate coronary arteries. Two patients had no significant ischemic ST changes in the 16 simultaneous lead ECG and no chest pain with PTCA. The six limb leads were recorded from Mason-Likar locations modified by moving them centrally on the anterior torso; the V leads were recorded in standard locations, except V_1 was moved to V_3R. Four extra leads were placed as follows: (1) left axilla, (2) left subcostal margin, (3) V_8, and (4) midback at the level of V_4–V_8. The left axillary and back leads discriminated diagonal and left circumflex (LCX) PTCAs from the others and from each other. V_6 showed ST elevation in all LCX PTCAs and in only 10% of left anterior descending occlusions. V_3R showed ST elevation in 82% of right coronary PTCAs. In 48/50 (96%) of PTCA occlusions the ST elevation was localized to the torso locations defined in Forward Model Simulations as specific for the arterial perfusion bed involved. These data strongly support the hypothesis that additional resolution and sensitivity to ischemic change is to be expected with a broader array of ECG leads. **Key words:** coronary angioplasty, multilead ECG.

The computer simulation of the total body surface electrocardiogram (ECG) that we developed over the past several years was constructed from measured cardiac and torso anatomy, resistivities, and electrophysiology.[1–5] The propogation wave of excitation in the normal human heart discretized at 1 mm^3 resolution was simulated[6] by the method of Huygens and projected to some 1,300 sites on a realistic inhomogenous torso that includes intracardiac blood mass and lungs. QRS criteria for infarct size resulting from these numerical experiments[7–9] have been validated in a series of clinical angiographic correlations[10,11] and classic pathoanatomic studies.[12–14] The model has since been enhanced[15] to include the simulation of the myocardial repolarization process by incorporating individual action potential waveforms into each 1 mm^3 "cell" of the fine-

From the Memorial Heart Institute of Long Beach, Long Beach, California and the Cardiology Department, Rancho Los Amigos Campus of the University of Southern California, Downey, California.

Supported in part by grant H071-87 from the Memorial Medical Center Foundation of Long Beach, California and contract F33615-87-D-609 with the US Air Force School of Aerospace Medicine, Brooks AFB, Texas.

grid model. During this same time period, Kornreich and associates reported discriminant function analysis of 150 lead body surface maps for the optimal lead location and ECG criteria to discriminate multilead ECGs of normals from those of patients with left ventricular hypertrophy, anterior infarct, inferior infarct, and non-Q infarct.[16–18] Optimal discrimination of these entities required leads in the upper and lower left anterior torso, right anterior torso, and on the back. This led to a recommended lead set of 20 simultaneous leads (20SL) and testable ECG criteria[19] for the detection (and quantification) of ischemia in any coronary artery distribution.

The purpose of this study is to report the use of a commercially available 16 simultaneous lead (16SL) system (The Marquette Case 12 with 4 extra V leads) in patients undergoing percutaneous transluminal coronary angioplasty (PTCA) at the Memorial Medical Center of Long Beach, California. These 16SL ECG data will be used to test the model predictions of the optimal lead locations for discriminating acute ischemia in each of three subdivisions of the left anterior descending (LAD) coronary artery, that is, distal LAD, main diagonal, and proximal LAD, and in the left circumflex (LCX) and the right coronary artery (RCA) distributions.

Methods

The study population consisted of 47 patients who had undergone elective PTCA as a part of their regular cardiology care at the Long Beach Memorial Heart Institute during the years 1987–1989. There were 35 men aged 40–80, mean age 60 years, and 12 women aged 49–75, mean age 64 years. All patients, with their attending cardiologist's agreement had given informed consent to have the 16-lead ECG recording done before and during the PTCA procedure. The recording was done with a commercially available system (the Marquette Case 12) using a version with 4 extra leads added to the standard 12-lead ECG recorder. The 12SL ECG is made up of 2 independent limb leads, from which the other 4 are computed, and 6 precordial leads for a total of 8 independent leads. Thus, when the 4 extra leads are included in the set as precordial leads there are 12 independent simultaneous leads which, when combined with the 4 computed ones, make up the 16SL ECG system. The system generates hard copy of the 16 leads on demand or in a preset protocol in 10-second episodes with a signal averaged median beat. It stores this data in magnetic form that can be downloaded on 3½" diskettes for later replay through the system. The amplitude of the ST-segment at an arbitrarily chosen interval after the J point is also routinely printed out with the waveforms for each episode, and plotted as a trend plot or a series of them at the end of each recording session. In this study the ST70 point, used in routine exercise testing at the Memorial Heart Institute, was chosen for all studies.

After careful skin preparation with acetone/alcohol and vigorous scrubbing, radiolucent electrodes were placed in the lead locations shown in Figure 1. Baseline recordings were initially taken with the limb leads on the extremities. These leads were then moved to the Mason-Likar locations[20] and were modified as follows: aVR and aVL were moved centrally to the third intercostal space (ICS) in the midclavicular line (MCL). aVF was moved from the left iliac crest to the seventh ICS in the MCL as shown in Figure 1. The four extra electrodes were placed as follows: LAX in the left axilla, LSC in the left subcostal area in the parasternal line at the level of aVF (seventh ICS in the MCL), V_8 on the back (opposite V_4) and MB5 in the midback (both the latter at the level of V_4–V_6). In order to evaluate the stability and reproducibility of the recordings and median beat methodology, two 16-lead ECG sets were recorded serially before any intervention. A baseline recording was repeated at each stage in the procedure, that is, before and after angiograms, catheter, and wire insertions, etc. The ECG was monitored on the system's CRT throughout the procedure. A set of recordings was made under the system's program control every 15 seconds during each occlusion with the angioplasty balloon and until the ECG was deemed visually stable postocclusion. At a later date all tracings were reviewed by two independent experienced readers who verified the onset-offset of waveforms and J point chosen by the algorithm. Any differences were resolved by consensus with a third reader.

One patient developed angina and classic ischemic ST depression with wire insertion past a tight obstruction in the proximal left anterior descending. The angina did not completely resolve with vasodilators despite evidence of contrast flow past the lesion around the guidewire. After a number of unsuccessful attempts to pass a balloon catheter past the lesion the procedure was abandoned and the patient sent for urgent bypass surgery. Since she did not have documented complete occlusion with the balloon catheter, she was not included in the tabulated results and will be discussed separately. Two additional patients with PTCA occlusion of the right coronary artery did not develop chest pain and exhibited no ST-T change during several sequential balloon occlusions of this artery. Since the goal of this

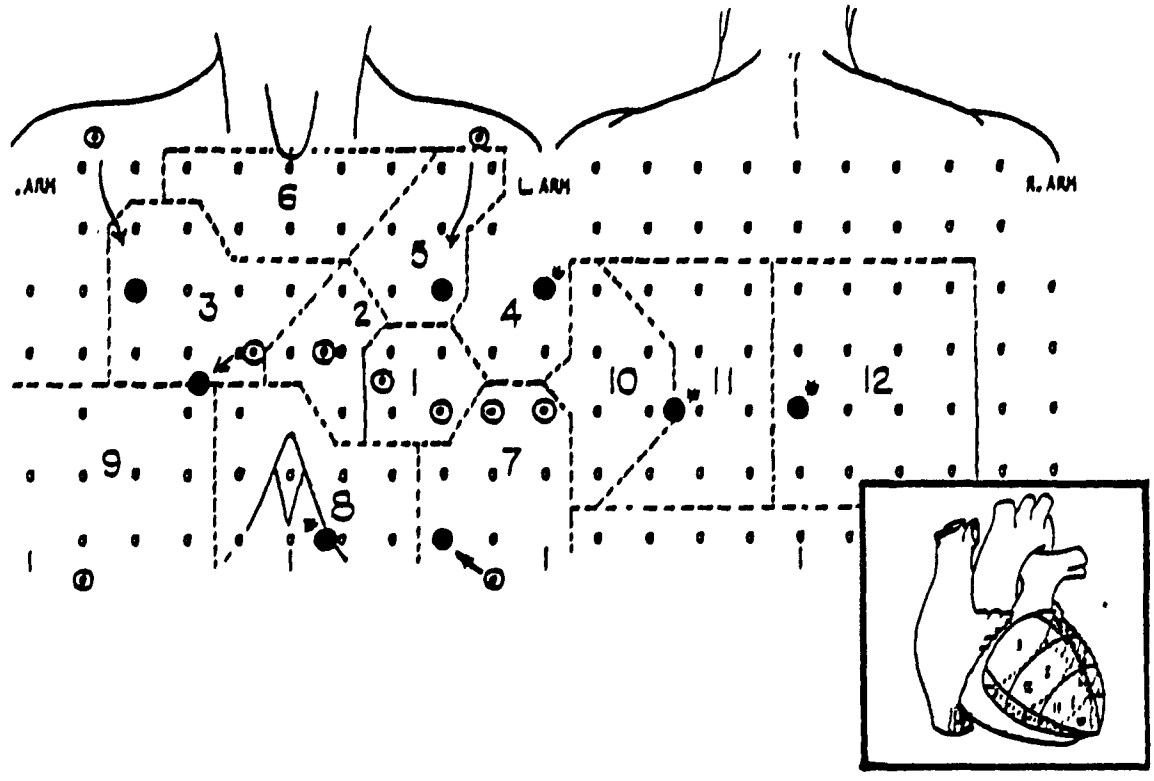

Fig. 1. The 16SL ECG lead locations on a body surface map. The Mason-Likar lead positions are modified by moving the arm leads to the third intercostal space (ICS) in the midclavicular line (MCL). The left leg (aVF) is moved to the seventh ICS in the MCL. The four additional leads shown by * are located in the left axilla (LAX), left subcostal (LSC) at the level of the new aVF, V_8, and midback (MB5) fifth anterior interspace at the V_4–V_8 level.

study was to test the ability of the multilead ECG to localize ischemic currents of injury when they occurred and there were no documented signs or symptoms of ischemia, these two patients were also excluded.

Of the remaining 44 patients, 4 had PTCA occlusion of 2 different arteries each for a total of 48 balloon occlusions. In 4 patients the occlusion was of the main diagonal branch of the left anterior descending (LAD) coronary, in 7 the occluded lesion was in the LAD distal to the main diagonal, and in 18 the LAD balloon occlusion was proximal; 8 PTCA occlusions were in the left circumflex (LCX), 5 were in the obtuse marginal, 1 in the distal LCX, and 2 proximal to the obtuse marginal. The PTCA occlusion of the right coronary artery (RCA) in 11 patients was in the midportion in 8, and in the distal RCA in 3. ST70 data were grouped and tabulated for 5 arterial subdivisions, 1 for each of the 3 LAD distributions, 1 for the LCX, and 1 for the RCA.

The individual verified amplitude of the ST70 segment in the median beat of the signal-averaged ECG was tabulated for each of the 16 leads and plotted on a worksheet showing the location of each lead in the body surface map format of Figure 1. Body surface equipotential map distributions of the ST70 from the median beats were constructed manually and compared to the left ventricular 12-segment distribution of the model projections of each segment displayed in this figure.

The ST70 amplitudes were then normalized to correct for the distance and/or proximity effects from the heart to each lead. For this purpose the scale factors for each lead defined in Table 1 were applied. The scale factors were derived by comparing the amplitude of a unit dipole located at the centroid of each LV segment in the simulation that was then projected to the thorax surface (Fig. 2) as described in earlier publications.[21–23] As seen in Figure 2 the anteroseptal and apical segments exhibit the largest proximity effects in the region of V_3–V_5. Thus the relative amplitude of the scale factor for each lead was established by taking the peak values of the anterior

Table 1. Model Scale Factors (Correction for Proximity Effects)

I: 2.0	2: 2.0	3: 2.0	aVR: 3.5	aVL: 2.0	aVF: 2.0
V_3R: 2.0	V_2: 1.4	V_3: 1.0	V_4: 1.0	V_5: 1.0	V_6: 1.5
LAX: 2.5	LSC: 2.5	V_8: 3.0	MB5: 3.0		

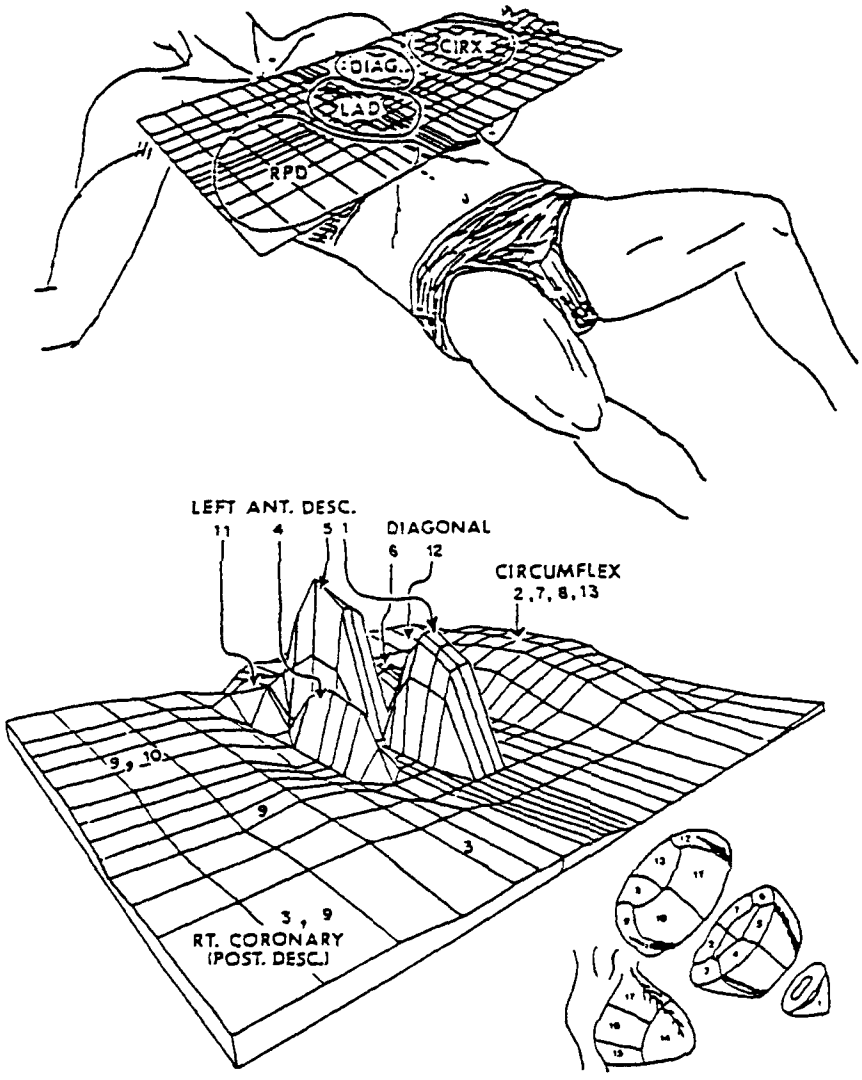

Fig. 2. The distribution of each unit dipole from 13 left ventricular segments shown in the lower right of the figure is projected onto the surface in the lower panel. The coronary artery supply to each segment is shown in the upper panel.

leads V_3, V_4, and V_5 as unity. The remaining Mason-Likar and torso leads were scaled upward to normalize them to the same relative local segment strength as the anteroseptal and apical segments. The scaled ST70 amplitudes were plotted on the body surface map format.

Results

Two hundred eighteen PTCA occlusions were performed in 46 patients ranging from 2 to 10 per patient; the average was 4.7 per patient. Four patients had PTCA of 2 vessels each. Inflation times were typically 1–2 minutes and varied from 0.25–5.0; the average was 1.6 minutes. The balloon occlusion showing the greatest departure of the median beat ST70 in the 16SL ECG from the baseline record prior to each occlusion was taken for analysis. The stability and reproducibility of the recording and median beat methodology was evaluated by examining the variance in the ST70 amplitudes in each of 2 sets of the 16 leads recorded at the beginning of each study. It was established from these data (16 × 46 pairs) that the 98% confidence limit of reproducibility of the measurement on the baseline tracings was ± 20μV. The two excluded asymptomatic subjects fell within these limits. The 48 PTCA balloon occlusions of individual coronary arteries in the remaining 44 patients each resulted in maximal elevation of the ST70 segment in leads predicted by the forward model to be specific for the arterial perfusion bed of the vessel occluded. The average ST changes and the ranges are shown graphically for the 16 leads in Figures 3 and 4 for each perfusion bed. The leads are ordered in groups corresponding to the right ventricle and the four left ventricular walls. The manually constructed

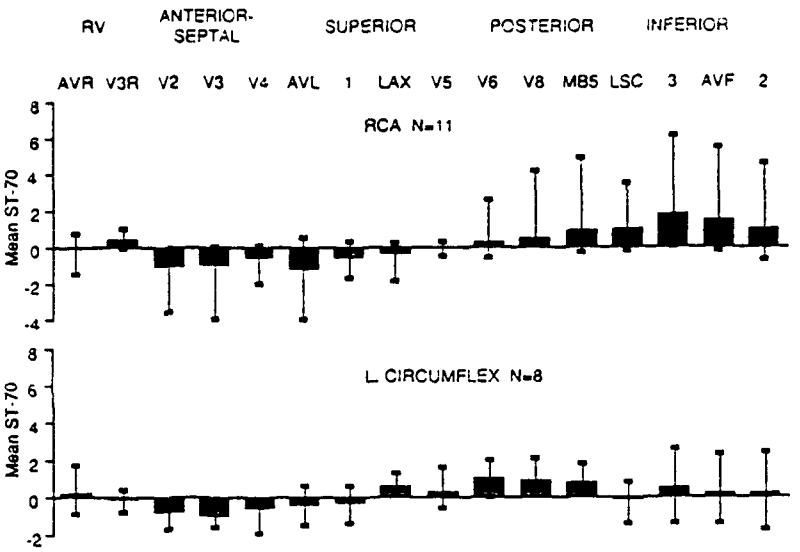

Fig. 3. Average change of ST70 and range (scale μV/100) during PTCA of the right coronary artery (RCA) and the left circumflex (LCX). The leads grouped from left to right correspond to the RV and four LV quadrants.

body surface equipotential maps from the median beat ST70 data were reviewed. It was noted that in leads more distant from the heart, even though there was significant ST change, the potential maxima were often displaced from the area projected for the local regions by the unit dipole transfer impedances. The amplitudes of the recorded ST70 segments in all leads were then scaled to the relative amplitude of the unit transfer impedances shown in Table 1. These data are summarized in Table 2. Maps constructed from these data confirm the forward model predictions. They were consistent with the hypothesis that,

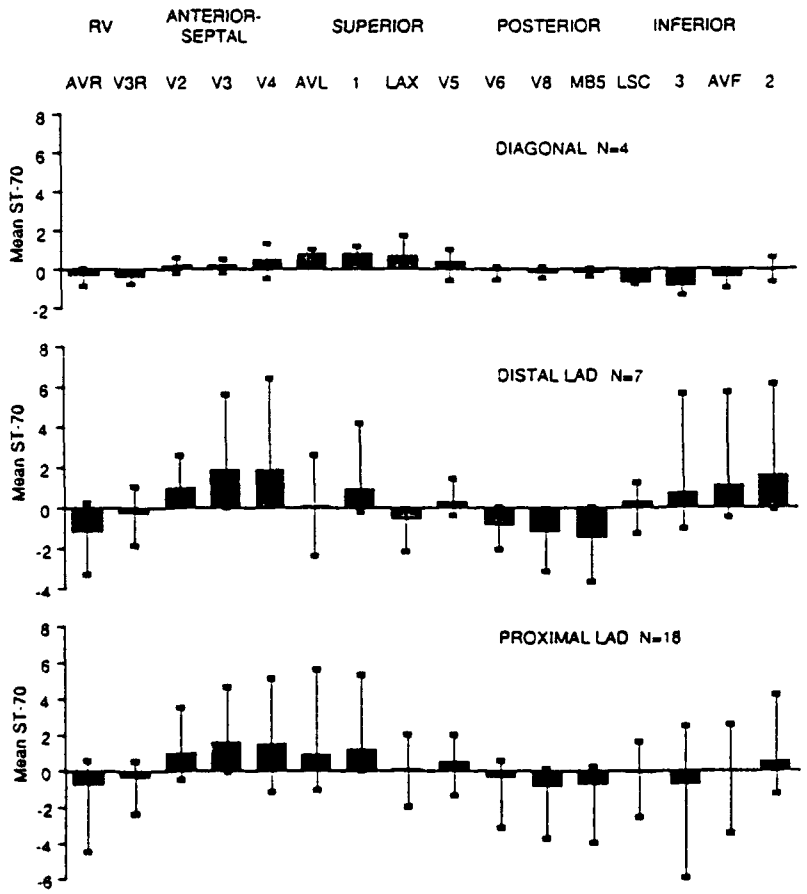

Fig. 4. ST70 change and range (scale μV/100) during PTCA of three left anterior descending (LAD) locations: (1) diagonal, (2) distal LAD, and (3) proximal LAD.

Table 2. PTCA Occlusion of Five Arterial Segments (48 Occlusions in 44 Patients): Mean Normalized Values and Ranges (μV/100) of ST70 for Each Lead

Lead	LAD Diagonal (n = 4)	LAD Distal (n = 7)	LAD Proximal (n = 18)	RCA (n = 11)	LCX (n = 8)
I	1.6 (1.0, 2.4)	1.8 (−0.4, 8.4)	2.5 (0.0, 10.6)	−1.3 (−3.4, 0.6)	−0.5 (−2.8, 1.2)
2	−0.1 (−1.4, 1.2)	3.1 (−0.2, 12.2)	0.8 (−2.6, 8.4)	2.1 (−1.4, 9.2)	0.4 (−3.4, 4.8)
3	−1.8 (−2.8, −1.0)	1.5 (−2.2, 11.2)	−1.9 (−12.0, 1.2)	3.5 (0.0, 12.2)	0.9 (−2.8, 5.2)
aVR	−1.1 (−3.2, 0.0)	−4.2 (−11.6, 0.7)	−2.8 (−15.8, 1.8)	−0.5 (−5.3, 2.5)	0.7 (−3.2, 6.0)
aVL	1.6 (1.2, 2.0)	0.2 (−4.8, 5.2)	1.9 (−2.2, 11.2)	−2.4 (−8.0, 1.0)	−0.9 (−3.0, 1.2)
aVF	−0.8 (−2.0, 0.0)	2.2 (−1.0, 11.4)	0.5 (−7.0, 3.4)	3.0 (−0.4, 11.0)	0.3 (−2.8, 4.6)
V_1R	−0.8 (−1.6, −0.4)	−0.7 (−3.8, 2.0)	−0.7 (−4.8, 1.0)	0.8 (−0.2, 2.0)	−0.2 (−1.6, 0.8)
V_2	0.3 (−0.3, 0.8)	1.4 (0.4, 3.6)	1.5 (−0.7, 4.9)	−1.5 (−5.0, −0.1)	−1.1 (−2.4, −0.1)
V_3	0.2 (−0.2, 0.5)	1.9 (0.0, 5.6)	1.7 (−0.1, 4.6)	−1.0 (−4.0, 0.0)	−1.0 (−1.6, −0.2)
V_4	0.5 (−0.5, 1.3)	1.9 (0.2, 6.4)	1.5 (−1.2, 5.1)	−0.6 (−2.0, 0.0)	−0.6 (−1.9, −0.1)
V_5	0.4 (−0.6, 1.0)	0.3 (−0.4, 1.4)	0.4 (−1.4, 2.0)	−0.1 (−0.5, 0.3)	0.3 (−0.6, 1.6)
V_6	−0.2 (−0.9, 0.2)	−1.4 (−3.2, 0.0)	−0.7 (−4.8, 0.8)	0.5 (−0.9, 3.9)	1.5 (0.0, 3.0)
LAX	1.8 (0.5, 4.3)	−1.6 (−5.5, −0.3)	0.1 (−5.0, 5.0)	−1.1 (−4.8, 0.5)	1.5 (0.5, 3.3)
LSC	−1.8 (−2.0, −1.5)	0.6 (−3.3, 3.0)	−0.4 (−6.5, 4.0)	2.5 (−0.5, 8.8)	−0.3 (−3.5, 2.0)
V_8	−0.6 (−1.5, 0.3)	−3.7 (−9.6, −0.3)	−2.8 (−11.4, 0.3)	1.6 (−0.9, 12.6)	2.8 (0.9, 6.3)
MB5	−0.6 (−1.2, 0.0)	−4.4 (−11.1, 0.0)	−3.0 (−12.0, 0.6)	2.6 (0.0, 14.7)	2.5 (0.6, 5.4)

when corrected in this way for local proximity effects, body surface ST70 change localizes to the region of the map specific for the local segment. The sum of the ST70 in each lead showing ST elevation of greater than the 20 μV reproducibility standard was accumulated for each of the five coronary arterial subsets described. The map of the ST70 change in each lead was computed and displayed as a three-dimensional plot on the perspective display of the surface map as shown in Figures 5 and 6. This was done to compare the relative ability of the local surface leads, scaled as described above, to predict the local current of injury from each of the five regions.

From a review of Table 2 it was noted that the peak amplitude of the scaled ST elevation (injury current) was seen in 1 or more of the 4 extra leads in 16 (33%) of 48 PTCAs in 44 patients. From a review of this data, and the perspective plots of Figure 5 and 6, the following observations can be made: (1) In the four patients with occlusion of the main diagonal branch of the LAD the maximal elevation of the mean ST occurred in the left axilla (180 μV) and modified aVL (160 μV) in the left upper chest with major ST depression in inferior leads, and minor ST depression or no significant change in back leads and V_6. (2) LAD occlusion distal to the first diagonal in seven patients produced local average ST elevation (220 μV) in modified aVF and similar amplitude changes (140 μV) in V_2, 190 μV in V_3, and V_4, minimal ST elevation in V_5, none in V_6, and significant depression in the left axilla and on the back. (3) PTCA occlusion of the LAD proximal to the first diagonal in 18 cases produced a combination of these effects with average ST elevation maximum in the left upper torso (190, 250 μV), 170 μV in V_3, 150 μV in V_4, and ST depression in V_6 and in back leads. (4) In the 8 patients with LCX occlusion the maximum of the averaged ST elevations was localized to the 2 back leads (280, 250 μV) with significant ST elevation in the left axilla and in V_6 (150 μV) and with ST depression in anterior leads. (5) RCA occlusion in 11 cases produced the maximal average ST elevation (350, 300 μV) in the inferior leads; there was significant involvement in the posterior leads in all but three. The expected mirror image ST depression in anterior leads V_2 and V_3 and the upper left anterior torso was also observed.

The one patient described earlier (but not included in the 44 just described) who developed persistent angina in the laboratory at the time of guidewire insertion through a proximal LAD stenosis had persistent ST depression associated with the angina throughout the rest of the procedure. ST depression occurred in anterior leads V_3–V_5 with the maximal change of 220 μV in V_4 and a classic downsloping ST-segment. The 18 patients with PTCA occlusion of the same artery all had ST elevation in the same leads. Intracoronary injection of contrast showed distal filling of the LAD around the guide wire. The pain and ST change responded incompletely to intravenous nitroglycerine drip, the ischemic ST-T changes persisted, and after several unsuccessful attempts to pass various balloon catheters past the obstruction the patient was referred to the surgeons for urgent bypass surgery, which was accomplished without incident.

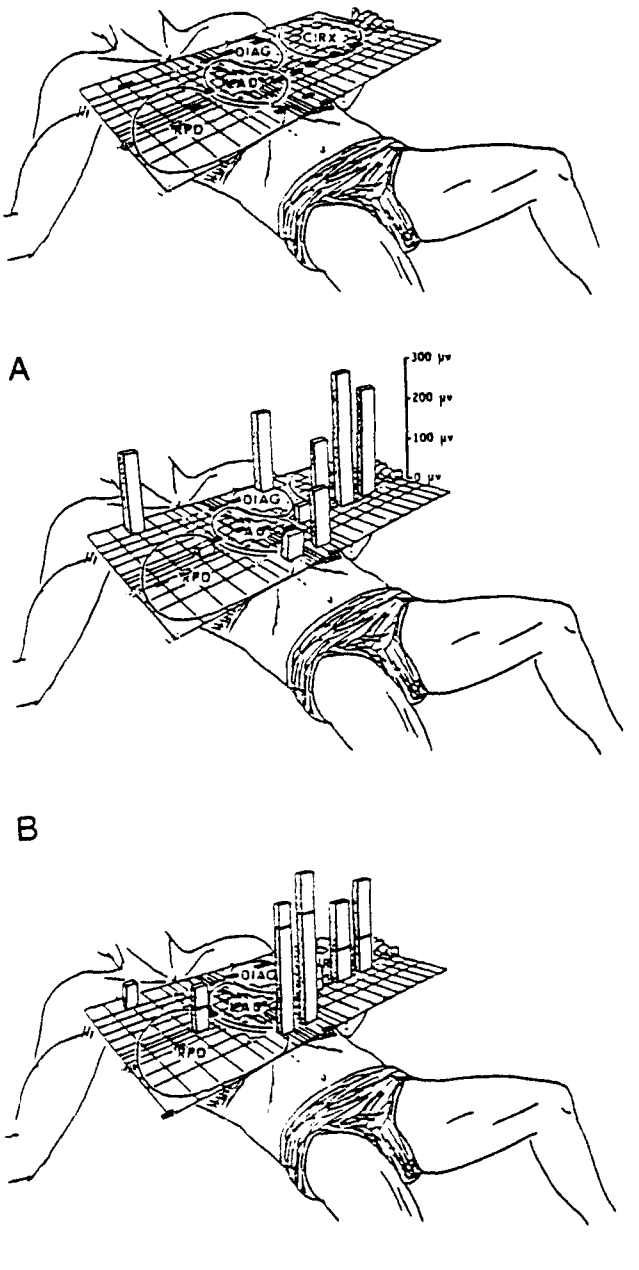

Fig. 5. (A) The 16 lead locations are shown as black rectangles on the body surface map. The mean ST70 elevations (positive potentials only) normalized for proximity effects during PTCA are shown in perspective as three-dimensional bars. Significant locations are seen for (B) the left circumflex in V_6 and in three extra leads (left axilla and two back leads) and (C) the right coronary artery in aVF and in three extra leads (subcostal and less in two back leads) and in V_1R.

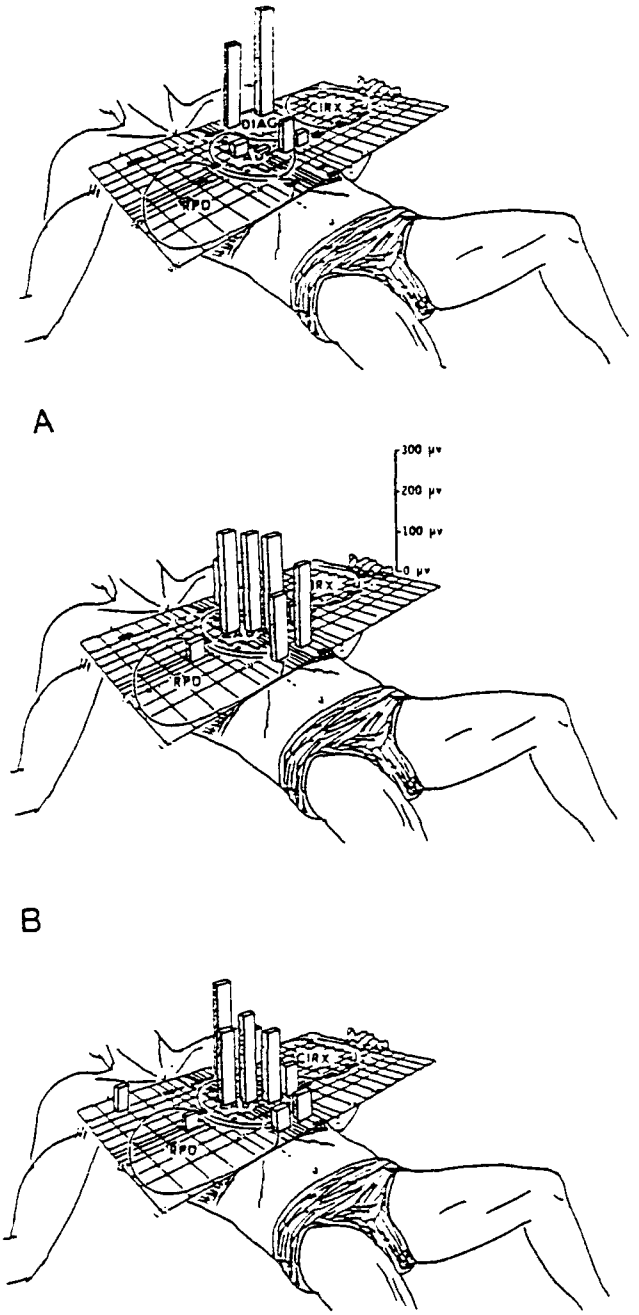

Fig. 6. Normalled mean ST70 elevation during PTCA (see Fig. 5 legend for description of three different left anterior descending (LAD) locations). Significant locations are seen for (A) diagonal LAD in aVL and left axilla; (B) distal LAD in V_2–V_4, aVF, and left subcostal lead; and (C) proximal LAD in a combination of the above leads.

Discussion

These data verify predictions from the forward model simulations and support the hypothesis that significant additional resolution and sensitivity to ischemic change is to be expected with a broader lead array. The extra lead in the axilla was strongly positive for ST injury with diagonal and circumflex occlusion in the present PTCA study. It separated this group from those with both distal LAD and RCA occlusion. The proposed 30SL lead array adds an extra lead on the left upper back 10 cm above the V_8 position. It is expected that it will discriminate between the LCX and the diagonal distributions and along with V_8 will be the most sensitive to ischemic changes in the obtuse marginal distribution. The midback lead was most sensitive to basal ischemia in both the RCA and LCX balloon occlusions but did not distinguish them well from each other. The new back leads at the V_8R position and high on the right back above it are expected to be most sensitive to ischemia (and/or infarct) in the high posterobasal regions of the left ventricle. These two leads also complete the back leads for the Grishman Cube System, which in the Rancho Database[24,25] was most sensitive to infarct and ischemia in this distribution.

It is of considerable interest that in the PTCA studies, lead V_6 ST changes consistently tracked with arterial distribution and ischemia to the posterior wall. In the study of 48 PTCAs in the population of 44 patients with demonstrable ischemic change with balloon occlusion, V_6 recorded significant ST elevation in 18/19 (95%) LCX and RCA occlusions. In the 11 distal LAD or diagonal occlusions none had ST elevation, but 7 had significant ST depression (from 30 to 320 μV) in V_6 as well as in both back leads. In the 18 proximal LAD occlusions, V_6 showed no demonstrable ST change in 3 cases in spite of major ST elevation in the anterior V leads; 12 had ST depression in V_6 ranging from 30 to 480 μV and even more ST depression on the back; and three had ST elevation of 30 to 80 μV. Thus, only 3/29 (10%) of the total patient group with LAD occlusion had demonstrable ST elevation ranging from 30 to 80 μV whereas 7 (24%) had no demonstrable change and 19 (66%) had ST depression ranging from 30 to 480 μV. It was also observed in the modeling studies of subendocardial ischemia (and/or infarction) that V_6 change (ST depression) was seen with ischemia in the obtuse marginal circumflex distribution, whereas with subendocardial ischemia in the distal LAD distribution there was little if any change or slight mirror image ST elevation in V_6. Only when there was major apical posterolateral ischemia extending well up toward or into the midregion did ST depression begin to appear in V_6.

The angioplasty studies demonstrated ST elevation in V_3R with occlusion of the RCA (9/11 PTCAs) and it was most marked when the occlusion was proximal to the acute marginal branch supplying the right ventricle. There was similar ST change (7/29 patients) with LAD occlusion associated with major change in V_2–V_4. These changes may represent ischemia of the base of the septum. From these observations, from the Kornreich studies, and from the simulation studies it is expected that the added leads on the right thorax will improve the sensitivity to ischemic change in the base of the septum and in the right ventricle. The V_4R lead in the new 30SL system completes the Grishman Cube and based on the Rancho database referred to above[24,25] should increase the sensitivity to both posterior wall change and the balance between it and the right ventricle.

There were three significant limitations to this study of local coronary artery balloon occlusion using the 16SL ECG system. First, the electrode array was limited to 4 sites added to the conventional 12-lead ECG and may have been suboptimal. The prior studies with the forward model had suggested that a 22-electrode set with 12 extra leads added to the standard 12 leads might be the optimal electrode array for detecting ischemia. The present study suggests the need for electrodes in the left upper back. The multigroup discriminant function studies of Kornreich et al. have also suggested the need for electrodes in the left lower flank. The possible location of these extra electrodes in the 30SL ECG currently being recorded in our laboratory is a synthesis of these three lines of study. The second major limitation of the present study is that except for the subjective chest pain and the ST changes on the 16SL ECG there is no independent objective measure of the degree of ischemia in the distal arterial perfusion bed produced by each of the coronary occlusions. The distribution of the coronary artery tree distal to the occlusions can be defined, but how much of this perfusion bed was ischemic, and the degree of that ischemia, was not systematically evaluated. The third limitation involves scaling of the waveforms and the ST70 amplitudes reported in this study. It was based on the assumption that torso proximity effects to the local regions of the heart during transmural ischemia can be accounted for by the unit transfer impedances from local regions during depolarization. Since the recovery process is distributed more widely over the heart at any given point in time than is excitation, the proximity effects from regional transmural ischemia may be less localized and thus less well rep-

resented by local transfer impedances from the simulation of excitation.

Future Directions

The increased spatial resolution from the added leads of the 30SL ECG system currently being implemented in our laboratory is expected to improve the detection of these ischemic changes when they occur. The 1 millisecond sampling rate and signal processing to reduce noise defines waveforms in significantly more detail. The higher resolution of each of these 30 individual waveforms that results from this processing and the ability to display them as 3-dimensional potential maps, discriminant function maps, spatial or temporal integral maps, etc., or as high-gain, high-resolution 12SL (or 36SL) ECGs and VCGs are expected to further improve the ability to detect these ischemic changes.

Using 30SL ECG data from the more extensive electrode array the forward model will be exercised to emulate the ECG changes of mild, moderate, and severe ischemic "injury" produced by several typical local PTCA occlusions and by exercise-induced ischemia in these same subjects. From these simulations we expect to refine our earlier recommendations for the optimal number and location of electrodes as well as the testable hypotheses for optimal criteria in these leads to detect "silent ischemia." We expect that the 30SL ECG does contain redundant electrode locations for this purpose. By the use of multivariate techniques on the sampled data, and judicious use of the forward simulation to define the anatomic and physical basis for the observed changes, it should be possible to define the minimal set of electrodes for application in the field that will optimize the detection of previously unrecognized coronary disease in asymptomatic subjects.

In the Framingham study[26-27] 25% of new infarcts that developed were clinically unrecognized and unsuspected until serial ECGs were recorded. A number of autopsy studies[28-30] have shown that when ECGs are also reviewed one third or more of old healed infarcts are clinically unsuspected and failed to meet conventional ECG criteria for infarction. They would be classified as completely "silent." From prior studies with high-resolution ECGs and VCGs,[7] serially recorded high-resolution multilead ECG/VCGs are now capable of identifying most, if not all, of these new "silent infarcts" that are not detected with routine serial 12-lead ECGs. The improved detection of "silent ischemia" can be expected with continued enhancement of the system as outlined above.

References

1. Selvester RH, Kalaba R, Kagiwada H et al: Simulated myocardial infarction with a mathematical model of the heart containing distance and boundary effects: vectorcardiography 1965, p. 403. In Hoffman I (ed): North Holland Publishing Co, Amsterdam, Netherlands, 1966
2. Selvester RH, Kalaba R, Collier CR et al: A digital computer model of the vectorcardiogram with distance and boundary effects: simulated myocardial infarction. Am Heart J 74:792, 1967
3. Selvester RH, Kirk WL, Pearson RB: Propagation velocities and voltage magnitudes in local segments of myocardium. Circ Res 27(4):619, 1970
4. Selvester RH, Solomon JC, Gillespie TL: Digital computer model of a total body ECG surface map: an adult male torso simulation with lungs. Circulation 38:684, 1968
5. Solomon JC, Selvester RH: Current dipole moment density of the heart. Am Heart J 81(3):351, 1971
6. Solomon JC, Selvester RH: Simulation of measured activation sequence in the human heart. Am Heart J 85(4):518, 1973
7. Selvester RH, Sanmarco ME: Infarct size in hi-gain, hi-fidelity serial VCGs and serial ventriculograms in patients with proven coronary artery disease. Proceedings of the 4th World Congress on Electrocardiography, 1978
8. Selvester RH, Wagner JO, Rubin HB: Quantitation of myocardial infarct size and location by electrocardiogram and vectorcardiogram, p. 31. In Snellen HA, Hemker HC, Hugenholtz DG, Van Bremmel JH (eds): Quantitation in Cardiology. Leiden University Press, Leiden, 1972
9. Selvester RH, Sanmarco ME, Solomon JC, Wagner GS: Methods of determining infarct size, ECG: QRS change, p. 23. In Wagner GS (ed): Myocardial Infarction: Measurement and Intervention. Martinus Nijhoff, The Hague, 1982
10. Palmeri ST, Harrison DG, Cobb FR et al: A QRS scoring system for assessing left ventricular function after myocardial infarction. N Engl J Med 306(1):4, 1982
11. Wagner GS, Freye CH, Palmeri ST et al: Evaluation of a QRS scoring system for estimating myocardial infarct size. I. specificity and observer agreement. Circulation 65:342, 1982
12. Ideker RE, Wagner GS, Ruth WK et al: Evaluation of a QRS scoring system for estimating myocardial infarct size. II. Correlation with quantitative anatomic findings for anterior infarcts. Am J Cardiol 49:1604, 1982
13. Roark SF, Ideker RE, Wagner GS et al: Evaluation of a QRS scoring system for estimating myocardial infarct size. III. correlation with quantitative anatomic findings for inferior infarcts. Am J Cardiol 51:382, 1983
14. Ward RM, White RD, Ideker RE et al: Evaluation of a QRS scoring system for estimating myocardial infarct size. IV. correlation with quantitative anatomic findings for posterolateral infarcts. Am J Cardiol 53:706, 1984

15. Solomon JC, Selvester RH, Tolan GD: An enhanced forward model of the heart. p. 146. In Bailey JJ (ed): Engineering Foundation Conference. Computerized Interpretation of the Electrocardiogram XI. Engineering Foundation, New York, 1986
16. Komreich F, Rautaharju PM, Warren JW et al: The contribution of body surface potential maps to optimal lead sets. Computerized Interpretation of the ECG IX. p. 182. In Selvester RH (ed): Proceedings of the Engineering Foundation Conference. Engineering Foundation, New York, 1983
17. Komreich F, Montague TJ, Rautaharju PM et al: Multigroup diagnosis of body surface potential maps. J Electrocardiol 22 (suppl):169, 1989
18. Komreich F, Montague TJ, Rautaharju PM et al: Identification of best electrocardiographic leads for diagnosing anterior and inferior myocardial infarction by statistical analysis of body surface potential maps. Am J Cardiol 58:863, 1986
19. Selvester RH, Solomon JC, Tolan GT: Fine grid computer simulation of QRS-T and criteria for quantitating regional ischemia. Computerized Interpretation of the ECG XII. J Electrocardiol 20(suppl) 1, 1987
20. Mason RE, Likar I: A new system of multiple-lead exercise electrocardiography. Am Heart J 71:196, 1966
21. Selvester RH, Solomon JC: Optimal ECG electrode sites and criteria for detection of asymtomatic coronary artery disease at rest and with exercise. USAF-SAM-TR-85-47, December 1985
22. Selvester RH, Gillespie TL: Simulated ECG surface map's sensitivity to local segments of myocardium in body surface mapping of cardiac fields. Adv Cardiol (Basel) 10:120, 1974
23. Selvester RH, Solomon JC, Pearson RB: ECG body surface map criteria for quantitating infarct, as derived from computer simulations. van Dam RT, van Oosterom A (eds): 3rd International Symposium on Body Surface Mapping. Martinus Nijhoff, Boston, 1985
24. Madrid WL, Sanmarco ME, Gaarder TG, Selvester RH: Circumflex occlusion and posterior myocardial infarction: diagnostic criteria and automated ECG analysis programs. Computerized Interpretation of the ECG XI. In Bailey JJ (ed): Proceedings Engineering Foundation Conferences. Engineering Foundation, New York, 1986
25. Selvester RH, Wagner GS, Ideker RE: Myocardial infarction. p. 565. In Macfarlane PW, Lawrie TD (eds): Comprehensive Electrocardiology. Pergamon Press, New York, 1989
26. Kannel WB, Feinleib M, Thomas RD: The unrecognized myocardial infarction. Geriatrics 25:75, 1970
27. Kannel WB, Abbott RD: Incidence and prognosis of unrecognized myocardial infarcton. New Engl J Med 311, 18:1144, 1984
28. Johnson WJ, Richard WPA, Burchell HB, Edwards JE: Unrecognized myocardial infarction. Arch Intern Med 103:253, 1959
29. Woods JD, Laurie W, Smith WG: The reliability of the electrocardiogram in myocardial infarction. Lancet 2:265, 1963
30. Cabin HS, Roberts WC: Quantitative comparison of extent of coronary narrowing and size of healed myocardial infarct in 33 necropsy patients with clinically recognized and in 28 with clinically unrecognized previous acute myocardial infarction. Am J Cardiol 50:677, 1982